

OPTIMIZATION OF SYNTHESIZED NANO CU-BASED CATALYST TO ENHANCE BIODIESEL PRODUCTION

ARVYVIE ABIE JAMIL

PERPUSTAKAAN
UNIVERSITI MALAYSIA SABAH

**THESIS SUBMITTED IN PARTIAL
FULFILLMENT FOR THE DEGREE OF MASTER
OF SCIENCE**

**FACULTY OF SCIENCE AND NATURAL
RESOURCES
UNIVERSITI MALAYSIA SABAH**

2016

UNIVERSITI MALAYSIA SABAH

BORANG PENGESAHAN STATUS TESIS

JUDUL: **OPTIMIZATION OF SYNTHESIZED NANO-CU BASED CATALYST TO ENHANCE BIODIESEL PRODUCTION**

IJAZAH: **MASTER OF SCIENCE (INDUSTRIAL CHEMISTRY)**

Saya **ARVYVIE ABIE JAMIL**, Sesi Pengajian **2013-2016**, mengaku membenarkan tesis Sarjana ini disimpan di Perpustakaan Universiti Malaysia Sabah dengan syarat-syarat seperti berikut:-

1. Tesis ini adalah hak milik Universiti Malaysia Sabah.
2. Perpustakaan Universiti Malaysia Sabah dibenarkan membuat salinan untuk tujuan pengajian sahaja.
3. Perpustakaan dibenarkan membuat salinan tesis ini sebagai bahan pertukaran antara institusi pengajian tinggi.
4. Sila tandakan (/)

SULIT

(Mengandungi maklumat yang berdarjah keselamatan atau kepentingan Malaysia seperti yang termaktub di dalam AKTA RAHSIA 1972)

TERHAD

(Mengandungi maklumat TERHAD yang telah ditentukan oleh organisasi/badan di mana penyelidikan dijalankan)

TIDAK TERHAD

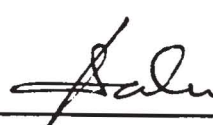


ARVYVIE ABIE JAMIL

Tarikh: 26 August 2016

Disahkan oleh,
NURULAIN BINTI ISMAIL

LIBRARIAN
UNIVERSITI MALAYSIA SABAH
(Tandatangan Pustakawan)



Dr. Jahimin A. Asik
Penyelia



UMS
UNIVERSITI MALAYSIA SABAH

CERTIFICATION

NAME : **ARVYVIE ABIE JAMIL**

MATRIK NO. : **MS1221017T**

TITLE : **OPTIMIZATION OF SYNTHESIZED NANO CU-BASED CATALYST TO ENHANCE BIODIESEL PRODUCTION**

DEGREE : **MASTER OF SCIENCE
(INDUSTRIAL CHEMISTRY)**

VIVA DATE : **29 JUN 2016**

CERTIFIED BY;

1. SUPERVISOR

Dr. Jahimin A. Asik

Signature



DR. JAHIMAN ASIK @ ABD. RASHID
Pemangku Timbalan Dekan (HEP & ALUMNI)
Fakulti Sains dan Sumber Alam
UNIVERSITI MALAYSIA SABAH

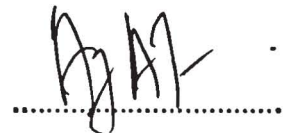
2. CO-SUPERVISOR

Rubia Idris

DECLARATION

I hereby declare that the material in this thesis is my own except for quotations, equations, summaries and references, which have been duly acknowledged.

26 August 2016



Arvyvie Abie Jamil

MS1221017T



ACKNOWLEDGEMENT

Firstly, I'm very thankful to Almighty god for his grace and give me the strength to complete this thesis. Secondly, I would like to express my deepest appreciation to my supervisor, Dr. Jahimin A. Asik and my co-supervisor, Miss Rubia Idris for the opportunity, financial support, supervision, invaluable advice, guidance and assistance throughout my research study. Not forget, all of industrial chemistry lecturer especially Mr. Tan Wei Hsiang. Their support and lessons were beyond the pages of the book and has made this work possible.

I wish to express my thanks to my dear family, Jamil Dangus, Suzie Fong, Amyjane, Aldyanie, Arvynecov, Annesonizye, Alldyonecov and Andrevcov for their support in spiritual, financial, encouragement and patience throughout my study. Not to forget my friend, Marycia Lisa who has given me a lot of motivation, her time and help in completing my study.

My sincere thanks to all the laboratory assistants and Science Officer of the Faculty Science and Natural Resources especially Mdm. Azimah, Mr. Recyheidy, Mr. Jerry, Mr. Sani, Mdm. Mala, Mdm. Marlenny, Mr. Taipin, Mr. Rahim and Mdm. Fairrendy for their guidance and technical support during the experimental process and instrumentation characterizations. Without them, I will never be able to complete this experiment successfully.

I'm also very thankful for the financial support from the Research Grant Scheme (Grant. No. RAG0042-TK-2013 and RAG0049-SG-2014) and My Master scholarship from the Ministry of Higher Education. Last but not least, thank you all to my lab-mates, Brian Brandon Bernard, Bryan Gindana and Florinna Tan for their help, sincere support, fruitful idea, constructive criticisms and unparalleled motivations that had contributed toward the realization of my thesis.

Arvyvie Abie Jamil

26 August 2016

ABSTRACT

Nowadays, the productions of biodiesel from renewable sources such as palm oil have been extensively studied due to the depletion of fossil fuel. The difficulties during the separation and purification of the homogeneous catalyst used in the production of biodiesel product led to the development of a heterogeneous catalyst. In this study, heterogeneous Cu-based catalyst was successfully synthesized using impregnation associated with sonochemical method. Two types of catalysts support (Al_2O_3 and MgO) were optimized and activated under two different activation conditions (air and nitrogen). Four parameters were optimized which are i) sonication time, ii) activation procedure (time and gas), iii) catalyst support (Al_2O_3 and MgO) and iv) metal loading (5 to 20 wt. %). Throughout the characterization data, it was confirmed that the optimized activation condition was at 90 minutes sonication time either 3 hours under nitrogen activation condition or 4 hours under air activation condition. From the XRD analysis, it was revealed the formation of CuO phase under air condition (20CuAA(4h)) produced smaller average crystal size of 23.6 nm compared to Cu phase produced under nitrogen condition (20CuAN(3h)), 30.1 nm. Moreover, effect of catalyst support has confirmed the MgO catalyst (10CuMA) produced highly dispersed of CuO phase with an average crystal size smaller than Al_2O_3 catalyst (10CuAA), 8.5 and 24.7 nm respectively. FESEM and TEM analysis also confirmed the MgO catalyst (10CuMA) produces small CuO nanocatalyst with lamella-like structure. The selected catalyst (5 to 20 wt. % of CuO/MgO catalyst) was performed under the transesterification reaction with a fixed parameter: 1 % w/w catalyst, temperature (65 °C), molar ratio of methanol to oil (10:1) and 6 hours reaction time. Throughout the study, 10 wt. % of CuO/MgO catalyst (10CuMA) showed a high catalytic activity with high conversion and high selectivity of palmitic acid, 97.2 % and 51.5 % respectively. From the XRD analysis, it was observed an average crystal size of CuO for 10CuMA catalyst was 8.5 nm. While from the BET analysis, it showed the 10CuMA catalysts is a mesoporous nanocatalyst ($133.9 \text{ cm}^3 \text{ g}^{-1}$) with an average pore diameter is less than 5 nm. FESEM and TEM analysis observed the 10CuMA catalyst consist of nanoparticles with lamella-like structure. From the thermal analysis, it was determined the 10CuMA catalyst consists of three stages of thermal decomposition with 29.4 % of weight loss and 70.6 % of ash residue. Overall the biodiesel produced by the 10CuMA catalyst meet the requirement of EN14214 standards with the acid value of less than 0.5 mg KOH g^{-1} and low iodine value.

ABSTRAK

Optimisasi Sintesis Pemangkin Nano Berasaskan Cu untuk Meningkatkan Pengeluaran Biodisel

Pada masa kini, kajian proses penghasilan biodisel dari sumber boleh diperbaharui contohnya minyak sawit amat rancak dilakukan memandangkan bahan api fossil semakin berkurangan. Kesukaran semasa pemisahan dan pembersihan pemangkin homogen yang digunakan dalam penghasilan biodisel telah membawa kepada perkembangan pemangkin heterogen. Dalam kajian ini, pemangkin heterogen berasaskan kuprum (Cu) telah berjaya disintesikan melalui kaedah impregnasi dengan bantuan sonokimia. Dua jenis sokongan pemangkin (Al_2O_3 dan MgO) telah dioptimumkan dan diaktifkan melalui dua jenis keadaan pengaktifan (udara dan nitogen). Empat parameter telah dioptimumkan seperti i) masa sonikasi, ii) prosedur pengakifan (masa dan gas), iii) sokongan pemangkin dan iv) muatan logam (5 ke 20 wt. %). Melalui data pencirian, ia dapat disahkan bahawa optimum pengaktifan adalah 90 minit sama ada 3 jam pengaktifkan dengan keadaan bernitogen atau 4 jam dengan keadaan berudara. Daripada analisis XRD, ia telah mendedahkan pembentukan fasa CuO di bawah keadaan berudara menghasilkan purata saiz hablur yang kecil 23.6 nm berbanding purata saiz hablur fasa Cu di bawah keadaan bernitogen, 30.1 nm. Selain itu, kesan sokongan pemangkin mengesahkan bahawa pemangkin MgO (10CuMA) menghasilkan peningkatan taburan hablur fasa CuO dengan purata saiz hablur yang kecil berbanding dengan pemangkin Al_2O_3 , masing-masing 8.5 dan 24.7 nm. Analisis FESEM dan TEM juga mengesahkan pemangkin MgO (10CuMA) menghasilkan hablur CuO nano-pemangkin yang kecil dengan struktur seakan kepingan. Pemangkin terpilih (5 ke 20 wt. % pemangkin CuO/MgO) telah menjalankan tindakbalas transesterifikasi dengan parameter malar: muatan mangkin pada 1 % w/w, suhu tindakbalas (65 °C), nisbah molar metanol kepada minyak (10:1) dan tempoh tindakbalas (6 jam). Sepanjang kajian, 10 wt. % pemangkin CuO/MgO (10CuMA) menunjukkan tindakbalas pemangkin tertinggi dengan penukaran yang tinggi dan pemilihan asid palmitik yang tinggi, masing-masing 97.2 % dan 51.5 %. Daripada analisis XRD, ia dapat diperhatikan purata saiz hablur untuk pemangkin 10CuMA ialah 8.5 nm. Manakala daripada analisis BET, ia menunjukkan pemangkin 10CuMA merupakan pemangkin nano mesoporous ($133.9 \text{ cm}^2\text{g}^{-1}$) dengan purata diameter liang kurang daripada 5 nm. Analisis FESEM dan TEM, menunjukkan pemangkin 10CuMA terdiri daripada nanopartikel dengan struktur seakan kepingan. Daripada analisis terma, ia menentukan pemangkin 10CuMA terdiri daripada tiga peringkat penguraian terma dengan 29.4 % kehilangan berat dan 70.6 % sisa abu. Keseluruhan, biodisel yang dihasilkan daripada pemangkin 10CuMA memenuhi keperluan standard EN 14214 dengan nilai asid kurang daripada 0.5 mg KOH g⁻¹.

TABLE OF CONTENTS

	Page
TITLE	i
DECLARATION	ii
ACKNOWLEDGEMENT	iv
ABSTRACT	v
ABSTRAK	vi
LIST OF CONTENTS	vii
LIST OF TABLES	xi
LIST OF FIGURES	xiii
LIST OF ABBREVIATIONS	xviii
LIST OF SYMBOLS	xxi
LIST OF APPENDIX	xxv
CHAPTER 1: INTRODUCTION	1
1.1 Overview of Biodiesel Technology	1
1.2 Problem Statement	3
1.3 Relevance of the Study	4
1.4 Objective of the Study	5
1.5 Scope of the Study	5
CHAPTER 2: LITERATURE REVIEW	7
2.1 Introduction of Catalyst	7
2.1.1 Metal Oxide Based Catalyst and Nanocatalyst	7
2.2 Catalyst Preparation	8
2.2.1 Co-precipitation	10
2.2.2 Sol-gel	11
2.2.3 Impregnation	12
2.2.4 Sonochemistry	14
2.3 Copper Based Catalyst Development and Its Application	15
2.3.1 Aluminum Oxide Based Catalyst	16
2.3.2 Magnesium Oxide Based Catalyst	16
2.4 Characterization Technique of Heterogeneous Catalysts	17
2.4.1 Crystallography Analysis	18

2.4.2	Morphology Analysis	19
2.4.3	Surface Area Analysis	20
2.4.4	Thermal Analysis	21
2.5	Biodiesel Production	22
2.5.1	Feedstock for Biodiesel Production	24
2.6	Process of Biodiesel Production	26
2.6.1	Direct Use and Blending	26
2.6.2	Microemulsification	27
2.6.3	Pyrolysis (Thermal Cracking)	27
2.6.4	Esterification	27
2.6.5	Transesterification	28
2.7	Transesterification Reaction Mechanisms	29
2.7.1	Homogeneous Catalyzed Transesterification	29
a.	Acid Catalyzed Processes	29
b.	Base-Catalyzed Processes	30
2.7.2	Heterogeneous Catalyzed Transesterification	32
2.8	Transesterification Parameters	32
2.9	Biodiesel Quality Control and Standards Development	34
2.9.1	Gas Chromatographic Analysis	34
2.9.2	Acid Value	35
2.9.3	Iodine Value	36
CHAPTER 3: METHODOLOGY		38
3.1	Overview of the Study	38
3.2	Experimental Design for Catalyst Synthesis	39
3.2.1	Optimization of Activation Condition	40
a.	Sonication Time	40
b.	Activation Procedure	41
3.2.2	Effect of Catalyst Support	42
3.2.3	Effect of Metal Loading	42
3.3	Catalysts Characterization	44
3.3.1	Crystallography Analysis	44
3.3.2	Morphology Analysis	46

a.	Scanning Electron Microscope (SEM) and Field Emission Scanning Electron Microscope (FESEM)	46
b.	Transmission Electron Microscope (TEM)	47
3.3.3	Surface Area Analysis	48
3.3.4	Thermal Analysis	49
3.4	Catalytic Reaction	50
3.4.1	Experimental Design for Transesterification Process of Palm Oil	50
3.4.2	Gas Chromatography Analysis	51
3.4.3	Acid Value	52
3.4.4	Iodine Value	53
CHAPTER 4: RESULTS AND DISCUSSION		54
4.1	Overview of Research Study	54
4.1.1	Formation of Cu-Based Nanocatalyst on Different Catalyst support	57
4.2	Optimization of Activation Condition	59
4.2.1	Sonication Time	59
a.	Crystallography Analysis	60
b.	Morphology Analysis	62
c.	Thermal Analysis	64
4.2.2	Activation Procedure	66
a.	Crystallography Analysis	67
b.	Morphology Analysis	69
c.	Thermal Analysis	71
4.3	Effect of Catalyst Support	75
4.3.1	Crystallography Analysis	75
4.3.2	Morphology Analysis	77
4.3.3	Surface Area Analysis	81
4.3.4	Thermal Analysis	84
4.3.5	Optimization of Catalyst Support	89
4.4	Effect of Metal Loading	92
4.4.1	CuO/MgO Catalyst Activated under Air Condition	92
a.	Crystallography Analysis	92

b.	Morphology Analysis	94
c.	Surface Area Analysis	99
d.	Thermal Analysis	101
4.4.2	Cu/MgO Catalyst Activated under Nitrogen Condition	104
a.	Crystallography Analysis	104
b.	Morphology Analysis	106
c.	Surface Area Analysis	110
d.	Thermal Analysis	111
4.4.3	Catalytic Performance	115
a.	Transesterification Process for CuO/MgO Catalyst Activated under Air Condition	115
b.	Transesterification Process for Cu/MgO Catalyst Activated under Nitrogen Condition	118
c.	Acid Value Assessment	120
d.	Iodine Value Assessment	122
CHAPTER 5: CONCLUSIONS AND FURTHER STUDY		124
5.1	Summary of the Study	124
5.2	Further Study	126
REFERENCES		127
APPENDIX		136

LIST OF TABLES

	Page
Table 1.1: Advantageous and disadvantageous of homogeneous and heterogeneous catalyst for biodiesel production	2
Table 2.1: Comparison properties of homogeneous and heterogeneous catalysts for the catalytic reaction	8
Table 2.2: Thermal analysis technique and method for heterogeneous catalyst	21
Table 2.3: Comparison of physical and chemical properties between diesel fuel and biodiesel	23
Table 2.4: Fatty acid distributions of some biodiesel feedstock	24
Table 2.5: Chemical structures of common fatty acids and their methyl esters	25
Table 2.6: Biodiesel standard based on EN14214 and ASTM D 6751	35
Table 2.7: Iodine value of plant oils	37
Table 3.1: Description of catalyst for the optimization of sonication time	40
Table 3.2: Description of catalyst for the optimization of activation procedure	41
Table 3.3: Description of catalyst for the effect of catalyst support	42
Table 3.4: Description of catalyst for the effect of metal loading	43
Table 4.1: Description of the catalyst sample with different catalyst support, metal loading and activation condition	58
Table 4.2: Comparative summary of nanocrystal size of nano CuO/Al ₂ O ₃ catalyst for the effect of sonication	61
Table 4.3: Summarized data from TGA and DTG thermogram of nano CuO/Al ₂ O ₃ for (a) 20CuAA(S30) (b)20CuAA(S60) (c) 20CuAA(S90) and (d) 20CuAA(S120)	66
Table 4.4: Comparative summary of nanocrystal size of nano Cu/Al ₂ O ₃ catalyst for the Effect of Activation Procedure	69

Table 4.5:	Summarized data from TGA and DTG thermogram of nano CuO/Al ₂ O ₃ catalyst for (a) 20CuAA(3h) (b) 20CuAA(4h) (b) 20CuAN(3h) and (d) 20CuAN(4h)	73
Table 4.6:	Comparative study of nanocrystal size of nano Cu-Based catalyst for the effect of catalyst support	77
Table 4.7:	Summarized data from TGA and DTG thermogram of nano Cu-based catalyst for (a) Pure Al ₂ O ₃ (b) 10CuAA (c) 10CuAN (d) Pure MgO (e) 10CuMA and (f) 10CuMN	86
Table 4.8:	Fatty acid methyl composition (%) and biodiesel yield (%) for the optimization of catalyst support	90
Table 4.9:	Comparative summary of nanocrystal size of nano CuO/MgO catalyst activated under air condition	94
Table 4.10:	Summarized data from TGA and DTG of nano CuO/MgO catalyst activated under air Condition for (a) 5CuMA (b) 10CuMA (b) 15CuMA and (d) 20CuMA	102
Table 4.11:	Comparative study of nanocrystal Size of nano Cu/MgO catalyst activated under nitrogen condition	105
Table 4.12:	Summarized data from TGA and DTG of nano Cu/MgO catalyst activated under nitrogen condition for (a) 5CuMN, (b) 10CuMN, (c) 15CuMN and (d) 20CuMN	114
Table 4.13:	Fatty acid methyl composition (%) and biodiesel yield (%) for MgO supported catalyst under air condition	116
Table 4.14:	Fatty acid methyl composition (%) and biodiesel yield (%) for MgO supported catalyst under nitrogen condition	120
Table 4.15:	Summarized data of acid value	121
Table 4.16:	Acid value of biodiesel from different raw material and catalyst	122
Table 4.17:	Summarized data of iodine value	123

LIST OF FIGURES

	Page
Figure 1.1: General transesterification process in biodiesel production	3
Figure 2.1: Catalytic reaction of supported metal oxide catalyst in which metal act as active site	9
Figure 2.2: Catalyst distribution by the impregnation method	13
Figure 2.3: Common characterization techniques for heterogeneous catalyst	17
Figure 2.4: Common transesterification process in the biodiesel production	22
Figure 2.5: Mechanisms of the acid-catalyzed transesterification of vegetable oils	30
Figure 2.6: Mechanisms of the base-catalyzed transesterification of vegetable oils	31
Figure 2.7: Reaction mechanisms for the heterogeneous catalyst of MgO.	32
Figure 3.1: Summarized of overall experimental procedures	39
Figure 3.2: Set up for the activation procedure	41
Figure 3.3: Various types of the catalyst characterization techniques	44
Figure 3.4: X-ray Diffraction (XRD) instrument	45
Figure 3.5: Vacuum and gold coating for Scanning Electron Microscope (SEM)	46
Figure 3.6: Scanning Electron Microscope (SEM) instrument	47
Figure 3.7: Transmission Electron Microscope (TEM) instrument	48
Figure 3.8: Thermogravimetry Analysis (TGA) instrument	49
Figure 3.9: Set up procedure for the transesterification process of palm oil by using nano-Cu based catalyst	51
Figure 3.10: Gas Chromatography Mass Spectroscopy (GCMS) instrument	52
Figure 4.1: Cu-oxalate/Al ₂ O ₃ catalysts before and after activation.	55
Figure 4.2: Cu-oxalate/MgO catalysts before and after activation.	56

- Figure 4.3: XRD pattern of nano Cu-Based catalyst for (a) pure Al₂O₃ 57
(b) air condition and (c) nitrogen condition
- Figure 4.4: XRD pattern of nano CuO/Al₂O₃ catalyst for (a) pure Al₂O₃ 61
(b) 20CuAA(S30) (c) 20CuAA(S60) (d) 20CuAA(S90) and (e)
20CuAA(S120)
- Figure 4.5: SEM image of nano CuO/Al₂O₃ catalyst (1 kx) (a) 63
20CuAA(S30) (b) 20CuAA(S60) (b) 20CuAA(S90) and (d)
20CuAA(S120)
- Figure 4.6: SEM image of nano CuO/Al₂O₃ catalyst (7 kx) (a) 63
20CuAA(S30) (b) 20CuAA(S60) (b) 20CuAA(S90) and (d)
20CuAA(S120).
- Figure 4.7: TGA and DTG thermogram of nano CuO/Al₂O₃ catalyst for 65
(a) 20CuAA(S30) (b) 20CuAA(S60) (b) 20CuAA(S90) and (d)
20CuAA(S120)
- Figure 4.8: XRD pattern of nano Cu/Al₂O₃ catalyst for (a) pure Al₂O₃ (b) 68
20CuAA(3h) (c) 20CuAA(4h) (d) 20CuAN(3h) and (e)
20CuAN(3h)
- Figure 4.9: SEM image of nano Cu/Al₂O₃ catalyst (1 kx) for (a) 70
20CuAA(3h) (b) 20CuAA(4h) (b) 20CuAN(3h) and (d)
20CuAN(4h)
- Figure 4.10: SEM image of nano Cu/Al₂O₃ catalyst (7 kx) (a) 20CuAA(3h) 70
(b) 20CuAA(4h) (b) 20CuAN(3h) and (d) 20CuAN(4h)
- Figure 4.11: TGA and DTG thermogram of nano CuO/Al₂O₃ catalyst for 72
(a) 20CuAA(3h) (b) 20CuAA(4h) (b) 20CuAN(3h) and (d)
20CuAN(4h)
- Figure 4.12: XRD pattern of nano Cu-based catalyst for (a) pure Al₂O₃ 76
(b) pure MgO (c) 10CuAA (d) 10CuAN (e) 10CuMA and (f)
10CuMN
- Figure 4.13: SEM image of nano Cu-based catalyst (1 kx) for (a) 10CuAA 78
(b) 10CuAN (c) 10CuMA and (d) 10CuMN
- Figure 4.14: SEM image of nano Cu-based catalyst (7 kx) for (a) 10CuAA 79
(b) 10CuAN (c) 10CuMA and (d) 10CuMN

- Figure 4.15: SEM image of nano Cu-based catalyst (a) 10CuAA (b) 79
10CuAN (c) 10CuMA and (d) 10CuMN 79
- Figure 4.16: N₂ adsorption-desorption isotherm and pore size distribution 82
of Nano Cu-based catalyst for (a) pure Al₂O₃ (b) 10CuAA
and (c) 10CuAN 82
- Figure 4.17: N₂ adsorption-desorption isotherm and pore size distribution 83
of Nano Cu-based catalyst for (a) pure MgO (b) 10CuMA
and (c) 10CuMN 83
- Figure 4.18: TGA and DTG thermogram of nano Cu-based catalyst for (a) 84
pure Al₂O₃ (b) 10CuAA and (c) 10CuAN 84
- Figure 4.19: TGA and DTG thermogram of nano Cu-based catalyst for (a) 85
pure MgO (b) 10CuMA and (c) 10CuMN. 85
- Figure 4.20: Biodiesel yield based on the composition of fatty acid 90
methyl esters for (a) Al₂O₃ supported and (b) MgO
supported catalyst 90
- Figure 4.21: XRD pattern of nano CuO/MgO catalyst activated under air 93
condition for (a) pure MgO (b) 5CuMA (c) 10CuMA (d)
15CuMA and (e) 20CuMA 93
- Figure 4.22: FESEM image of nano CuO/MgO catalyst under air condition 95
(10 kx) for (a) 5CuMA (b) 10CuMA (c) 15CuMA and (d)
20CuMA 95
- Figure 4.23: FESEM image of nano CuO/MgO catalyst under air condition 96
(50 kx) for (a) 5CuMA (b) 10CuMA (c) 15CuMA and (d)
20CuMA 96
- Figure 4.24: TEM image of nano CuO/MgO catalyst under air condition 96
for (a) 5CuMA (b) 10CuMA (c) 15CuMA and (d) 20CuMA 96
- Figure 4.25: FESEM image (left) and EDX (right) of nano CuO/MgO 97
catalyst under air condition for (a) 5CuMA (b) 10CuMA (c)
15CuMA and (d) 20CuMA 97
- Figure 4.26: N₂ adsorption-desorption isotherm and pore size distribution 100
of nano CuO/MgO catalyst activated under air condition for
(a) 5CuMA (b) 10CuMA (c) 15CuMA and (d) 20CuMA 100

- Figure 4.27: TGA and DTG thermogram of nano CuO/MgO catalyst 101 activated under air condition for (a) 5CuMA (b) 10CuMA (b) 15CuMA and (d) 20CuMA
- Figure 4.28: XRD pattern of nano Cu/MgO catalyst activated under 105 nitrogen condition for (a) pure MgO (b) 5CuMN (c) 10CuMN (d) 15CuMN and (e) 20CuMN
- Figure 4.29: FESEM image of nano Cu/MgO catalyst under N₂ condition 107 (10 kx) for (a) 5CuMN (b) 10CuMN (b) 15CuMN and (d) 20CuMN
- Figure 4.30: FESEM image of nano Cu/MgO catalyst under N₂ condition 108 (50 kx) for (a) 5CuMN (b) 10CuMN (b) 15CuMN and (d) 20CuMN
- Figure 4.31: TEM image of nano Cu/MgO catalyst under nitrogen 108 condition for (a) 5CuMN (b) 10CuMN (b) 15CuMN and (d) 20CuMN.
- Figure 4.32: FESEM image (left) and EDX (right) of nano Cu/MgO 109 catalyst under nitrogen condition for (a) 5CuMN (b) 10CuMN (b) 15CuMN and (d) 20CuMN catalyst
- Figure 4.33: N₂ adsorption-desorption isotherm and pore size distribution 111 of nano Cu/MgO catalyst activated under nitrogen condition for (a) 5CuMN (b) 10CuMN (c) 15CuMN and (d) 20CuMN
- Figure 4.34: TGA and DTA thermogram of nano Cu/MgO catalyst 112 activated under nitrogen condition for (a) 5CuMN (b) 10CuMN (b) 15CuMN and (d) 20CuMN
- Figure 4.35: Effect of the reaction conditions on biodiesel yield and fatty 116 acid methyl esters compositions on CuO/MgO catalyst activated under air condition
- Figure 4.36: Effect of the reaction conditions on biodiesel yield and fatty 119 acid methyl esters compositions on Cu/MgO catalyst activated under nitrogen gas condition
- Figure 4.37: Acid value of biodiesel sample for (a) CuO/MgO activated 121 under air condition and (b) CuO/MgO activated under nitrogen condition

Figure 4.38: Iodine value of the biodiesel sample for (a) CuO/MgO 123 activated under air condition and (b) CuO/MgO activated under nitrogen condition

LIST OF ABBREVIATIONS

AV	- Acid value
BET	- Brunauer-Emmet-Teller
CPO	- Crude palm oil
DTA	- Differential thermal analysis
DTG	- Differential thermogravimetry
EDX	- Energy dispersive X-ray
EM	- Electron microscopy
FAME	- Fatty acid methyl ester
FESEM	- Field emission scanning electron microscope
FFA	- Free fatty acid
FWHM	- Full width at half maximum
GC	- Gas chromatography
GCMS	- Gas chromatography mass spectroscopy
h	- Hour
IV	- Iodine value
JCPDS	- Joint Committee on Powder Diffraction Standards
min	- Minute
N₂	- Nitrogen gas
NLDFT	- Non-local Density Functional Theory
SEM	- Scanning electron microscope

TEM	- Transmission electron microscope
TG	- Thermogravimetry
XRD	- X-ray Diffraction
5CuAA	- 5 % Cu/Al ₂ O ₃ under air condition
5CuAN	- 5 % Cu/Al ₂ O ₃ under nitrogen condition
5CuMA	- 5 % CuO/MgO under air condition
5CuMN	- 5 % Cu/MgO under nitrogen condition
10CuAA	- 10 % CuO/Al ₂ O ₃ catalyst under air condition
10CuAN	- 10 % Cu/Al ₂ O ₃ catalyst under nitrogen condition
10CuMA	- 10 % CuO/MgO under catalyst air condition
10CuMN	- 10 % Cu/MgO under catalyst nitrogen condition
15CuAA	- 15 % CuO/Al ₂ O ₃ under air condition
15CuAN	- 15 % Cu/Al ₂ O ₃ under nitrogen condition
15CuMA	- 15 % CuO/MgO under air condition
15CuMN	- 15 % Cu/MgO under nitrogen condition
20CuAA	- 20 % CuO/Al ₂ O ₃ under air condition
20CuAN	- 20 % Cu/Al ₂ O ₃ under nitrogen condition
20CuMA	- 20 % CuO/MgO under air condition
20CuMN	- 20 % Cu/MgO under nitrogen condition
20CuAA(S30)	- 30 min of sonication time on Cu-oxalate/Al ₂ O ₃ catalyst
20CuAA(S60)	- 60 min of sonication time on Cu-oxalate/Al ₂ O ₃ catalyst
20CuAA(S90)	- 90 min of sonication time on Cu-oxalate/Al ₂ O ₃ catalyst

- 20CuAA(S120)** - 120 min of sonication time on Cu-oxalate/Al₂O₃ catalyst
- 20CuAA(3h)** - 3h activation under air condition on Cu-oxalate/Al₂O₃ catalyst
- 20CuAA(4h)** - 4h activation under air condition on Cu-oxalate/Al₂O₃ catalyst
- 20CuAN(3h)** - 3h activation under N₂ condition on Cu-oxalate/Al₂O₃ catalyst
- 20CuAN(4h)** - 4h activation under N₂ condition on Cu-oxalate/Al₂O₃ catalyst

LIST OF SYMBOLS

°C	-	Degree celcius
°C/min	-	Degree celcius per minute
°	-	Degree
%	-	Percentage
Å	-	Angstrom
β	-	Pure diffraction broadening of a peak at half height (in radian).
λ	-	Wavelength of the diffraction beam (1.5418Å)
ε	-	Angle of reflection or position of the peak in 2θ
µm	-	Micrometre
µL	-	Microlitre
2θ	-	Two theta
A	-	Biodiesel sample titration volume in millilitres
Al₂O₃	-	Aluminium Oxide
B	-	blank titration volume in millilitres
B2	-	2 % biodiesel and 98% petroleum diesel fuel
B5	-	5 % biodiesel and 95% petroleum diesel fuel
B7	-	7 % biodiesel and 93 % petroleum diesel fuel
B20	-	20 % biodiesel and 80 % petroleum diesel fuel
B100	-	100 % biodiesel

c	-	Isothermal constant.
cc/g	-	Cubic centimeter per gram
C	-	Carbon
C_{KOH}	-	Concentration of KOH expressed in mol L ⁻¹
C_{Na₂S₂O₃}	-	Concentration of sodium thiosulphate solution in mol L ⁻¹
C 8:0	-	Caprylic or Caprylate
C 10:0	-	Capric or Caproate
C 12:0	-	Lauric or Laurate
C 14:0	-	Myristic or Myristate
C 16:0	-	Palmitic or Palmitate
C16:1	-	Palmitoleic or Palmitoleate
C 18:0	-	Stearic or Stearate
C 18:1	-	Oleic or Oleate
C 18:2	-	Linoleic or Linoleate
C 18:3	-	Linolenic or Linolenate
C20:0	-	Arachidic or Arachidate
C 20:1	-	Eicosenoic or Eicosenoate
C 22:0	-	Behenic or Behenate
C 22:1	-	Eurcic or Eurcate
CaO	-	Calcium oxide
Cu	-	Copper
CuC₂O₄	-	Copper Oxalate

REFERENCE

- Ahmad, F., Khan, A.U. & Yasar, A. 2013. Transesterification of oil extracted from different species of algae for biodiesel production. *African Journal of Environmental Science and Technology.* **7**: 358-364.
- Akbari, B., Tavandashti, M.P. & Zandrahimi, M. 2011. Particle size characterization of nanoparticles- a practical approach. *Iranian Journal of Materials Science & Engineering.* **8** (2): 48-56.
- Aricetti, J.A. & Tubiono, M. 2012. A green and simple visual method for the determination of the acid-number of biodiesel. *Fuel.* **95**: 659-661.
- Athar, T., Hakeem, A. & Ahmed, W. 2012. Synthesis of MgO nanopowder via non aqueous sol-gel method. *Advanced Science Letters.* **5**: 1-3.
- Baco-Carles, V., Datas, L. & Tailhades, P. 2011. Copper nanoparticles prepared from oxalic precursors. *ISRN Nanotechnology.* **2011**:1-7.
- Behnoudnia, F. & Dehghani, H. 2013. Copper (II) oxalate nanospheres and its usage in preparation of Cu(OH)₂, Cu₂O and CuO nanostructures: synthesis and growth mechanism. *Polyhedron.* **56**: 102-108.
- Bhunia, P., John, R.P., Yan, S., Tyagi, R.D. & Surampalli. 2010. Algae Biodiesel Production: Challenges and Opportunities. In Khanal, S.K., Surampalli, R.Y., Zhang, T.C., Lamsal, B.P., Tyagi, R.D. & Kao, C.M. *Bioenergy and Biofuel from Biowastes and Biomass*, pp. 313-345. United States of America: American Society of Civil Engineer.
- Bowker, M. 2008. *The Basis and Applications of Heterogeneous Catalysis*. New York: Oxford University Press.

- Carrero, A. & Pérez, Á. 2012. Advances in biodiesel quality control, characterization and standards development. In Luque, R. & Melero, J.A. (e.d.). *Advances in Biodiesel Production Processes and Technologies*, pp. 91-130. UK: Woodhead Publishing.
- Chhetri, A.B. Watts, K.C. & Islam, M.R. 2008. Waste cooking oil as an alternate feedstocks for biodiesel production. *Energies*. **1** (1): 3-18.
- Chopra, A., Tewari, A.K., Vatsala, S., Kumar, R., Sarpal, A.S. & Basu, B. 2011. Determination of polyunsaturated fatty esters (PUFA) in biodiesel by GC/GC-MS and ¹H-NMR techniques. *J Am Oil Chem Soc*. **88**: 1285-1296.
- Cui, H., Wu, X., Chen, Y., Zhang, J. & Boughton, R.I. 2015. Influence of copper doping on chlorine adsorption and antibacterial behavior of MgO prepared by co-precipitation method. *Materials Research Bulletin*. **61**: 511-518.
- Dayananda, D., Sarva, V.R., Prasad, S.V., Arunachalam, J., Parameswaran, P. and Gosh, N.N. 2015. Synthesis of MgO particle loaded mesoporous Al₂O₃ and its defluoridation study. *Applied surface Science*. **329**: 1-10.
- de Jong, K.P. 2009. General aspects. In de Jong, K.P. (e.d.). *Synthesis of Solid Catalyst*, pp. 56-82. Weinheim: WILEY-VCH Verlag GmbH & Co.
- Demirbas, A. 2008. Relationships derived from physical properties of vegetable oil and biodiesel fuels. *Fuel*. **87**: 1743-1748.
- Deng, X., Fang, Z., Liu, Y. & Yu, C. 2011. Production of biodiesel from Jatropha oil catalyzed by nanosized solid basic catalyst. *Energy*. **36** (2): 777-784.
- Eevera, T., Rajendran, K. & Saradha, S. 2009. Biodiesel production process optimization and characterization to assess the suitability of the product for varied environmental conditions. *Renewable Energy*. **34**: 762-765.
- El-Molla, S.A., Abdel-all, S.M. & Ibrahim, M.M. 2009. Influence of precursor of MgO and preparation conditions on the catalytic dehydrogenation of iso-propanol over CuO/MgO catalysts. *Journal of Alloys and Compounds*. **484** (3): 280-285.

- Fan, M. Zhang, P. & Ma, Q. 2012. Enhancement of biodiesel synthesis from soybean oil by potassium fluoride modification of calcium magnesium oxides catalyst. *Bioresource Technology*. **104**: 447-450.
- Franco, F., Pérez-Maqueda, L.A. & Pérez-Rodríguez, J.L. 2004. The effect of ultrasound on the particle size and structural disorder of a well-ordered kaolinite. *Journal of Colloid and Interface Science*. **274**: 107-117.
- Gerpen, J.V. & Knothe, G. 2005. Biodiesel Production. In Knothe, G., Gerpen, J.V. & Krahl, J. (e.d.). *The Biodiesel Handbook*, pp. 26-41. USA: AOCS Press.
- Gupta, P. & Ramrakhiani, M. 2009. Influence of the particle size on the optical properties of CdSe nanoparticles. *The Open Nanoscience Journal*. **3**: 15-19.
- Hagens, J. 2006. *Industrial Catalysis* (2nd edition). Weinheim: WILEY-VCH Verlag GmbH & Co.
- Haq, I. & Haider, F. 2009. Synthesis and characterization of uniform fine particles of copper oxalate. *Materials Letters*. **63** (27): 2355-2357.
- Islam, A., Taufiq-Yap, Y.H., Chu, C. & Chan, E. 2013. Studies on design of heterogeneous catalysts for biodiesel production. *Process Safety and Environmental Protection*. **91** (1-2): 131-144.
- Jan, T., Iqbal, J., Ismail, M., Badshah, N., Mansoor, Q., Arshad, A. & Ahkam, Q.A. 2014. Synthesis, physical properties and antibacterial activity of metal oxides nanostructures. *Materials Sciences in Semiconductor Processing*. **21**: 154-160.
- Jeswani, H.K. & Azapagic, A. 2012. Life cycle sustainability assessment of second generation biodiesel. In Luque, L. & Melero, J.A. *Advances in Biodiesel Production*, pp. 13-31. United Kingdom: Woodhead Publishing.
- Jia, Z., Yue, L., Zheng, Y. & Xu, Z. 2008. The convenient preparation of porous CuO via copper oxalate precursor. *Materials Research Bulletin*. **43** (8-9): 2434-2440.

- Jiang, H., Bongard, H., Schmidt, W. & Schuth, F. 2012. One-pot synthesis of Cu/ γ -Al₂O₃ as bifunctional catalyst for direct dimethyl ether synthesis. *Microporous and Mesoporous Materials*. **164**: 3-8.
- Johari, A., Nyakuma, B.B., Nor, S.H.M., Mat, R., Hashim, H., Ahmad, A., Zakaria, Z.Y. & Abdullah, T.A.T. 2015. The challenges and prospects of palm oil based biodiesel in Malaysia. *Energy*. **81**: 255-261.
- Jr, F.A.U. 2010. *Biofuels from Plants Oils*. Indonesia: ASEAN Foundation.
- Juan, J.C., Kartika, D.A., Wu, T.K. & Taufiq-Yap, Y.H. 2011. Biodiesel production from jatropha oil by catalytic and non-catalytic approaches: An overview. *Bioresource Technology*. **102** (2): 452-460.
- Kanagasabapathi, N., Balamurugan, K. & Mayilsamy, K. 2012. Wear and thermal conductivity studies on nano particle suspended soya bean lubricant. *Journal of Scientific & Industrial Research*. **71**: 492-495.
- Knothe, G. 2005. Analytical Methods for Biodiesel. In Knothe, G., Gerpen, J.V. & Krahl, J. (e.d.). *The Biodiesel Handbook*, pp. 62-75. USA: AOCS Press.
- Kulkarni, N.V., Karmakar, S., Asthana, S.N., Nawale, A.B., Sheikh, A., Patole, S.P., Yoo, J.B., Mathe, V.L., Das, A.K. & Bhoraskar, S.V. 2011. Study on growth of hallow nanoparticles of alumina. *Journal Material Science*. **46**: 2212-2220.
- Landau, M. V. 2009. Sol-Gel processing. In de Jong, K.P. (e.d.). *Synthesis of Solid Catalyst*, pp. 83-109. Weinheim: WILEY-VCH Verlag GmbH & Co.
- Lande, M., Navgire, M., Rathod, S., Katkar, S., Yelwande, A. & Arbad, B. 2012. An effective green synthesis of quinoxaline derivatives using carbon-doped MoO₃-TiO₂ as a heterogeneous catalyst. *Journal of Industrial and Engineering Chemistry*. **18**: 277-282.
- Lee, J. & Saka, S. 2010. Biodiesel production by heterogeneous catalysts and supercritical technologies. *Bioresource Technology*. **101** (19): 7191-7200.

- Lee, D.W. & Yoo, B.R. 2014. Advanced metal oxide (supported) catalysts: Synthesis and applications. *Journal of Industrial and Engineering Chemistry*. **20** (6): 3947-3959.
- Lekhal, A. Glasser, B.J. & Khinast, J.G. 2001. Impact of drying on the catalyst profile in supported impregnation catalysts. *Chemical Engineering Science*. **56**: 4473-4478.
- Lele, S. 2008. *Biodiesel and Jatropha Cultivation*. India: Agrobios (India).
- Lim, S. & Teong, L.K. 2010. Recent trends, opportunities and challenges of biodiesel in Malaysia. *Renewable and Sustainable Energy Reviews*. **14**: 938-954.
- Lim, W.T.L., Zhong, Z. & Borgna, A. 2009. An effective sonication-assisted reduction approach to synthesize highly dispersed Co nanoparticles on SiO₂. *Chemical Physics Letters*. **471** (1-3): 122-127.
- Lin, L., Cunshan, Z., Vittayapadung, S., Xiangqian, S. & Mingdong, D. 2011. Opportunities and challenges for biodiesel fuel. *Applied Energy*. **88** (4): 1020-1031.
- Ling, P., Li, D. & Wang, X. 2012. Supported CuO/Al₂O₃ as heterogeneous catalyst for synthesis of diaryl ether under ligand-free conditions. *Journal of Molecular Catalysis A: Chemical*. **357**: 112-116.
- Liu, H., Su, Ling, Shao, Y. & Zou, L. 2012. Biodiesel production catalyzed by cinder supported CaO/KF particle catalyst. *Fuel*. **97**: 651-657.
- Lok, M. 2009. Coprecipitation. In de Jong, K.P. (e.d.). *Synthesis of Solid Catalyst*, pp. 135-151. Weinheim: WILEY-VCH Verlag GmbH & Co.
- Luque, R. & Melero, J.A. 2012. Introduction to advanced biodiesel production. In Luque, R. & Melero, J.A. *Advances in Biodiesel Production Processes and Technologies*, pp. 1-9. UK: Woodhead Publishing.

- Ma, L., Liu, Y., Shi, Q., Zhao, Q. & Gao, Z. 2009. Effect of Cu addition in reduction of MgO content for the synthesis of MgB₂ through sintering. *Journal of Alloys and Compounds.* **471:** 105-108.
- Ma, Z. & Zaera, F. 2006. Characterization of heterogeneous catalyst. In Richards, R. (e.d.). *Surface and Nanomolecular Catalysis*, pp. 1-37. New York: CRC Press Taylor & Francis Group.
- Mageshwari, K., Mali, S.S., Sathyamoorthy, R. & Patil, P.S. 2013. Template-free synthesis of MgO nanoparticles for effective photocatalytic applications. *Powder Technology.* **249:**456-462.
- Marceau, E., Carrier, X. & Che, M. 2009. Impregnation and drying. In de Jong, K.P. (e.d.). *Synthesis of Solid Catalyst*, pp. 1-11. Weinheim: WILEY-VCH Verlag GmbH & Co.
- Mofijur, M., Masjuki, H.H., Kalam, M.A., Liaquat, A.M., Shahabuddin, M. & Varman, M. 2012. Prospects of biodiesel from Jatropha in Malaysia. *Renewable and Sustainable Energy Review.* **16** (7): 5007-5020.
- Niesz, K. & Morse, D.E. 2010. Sonication-accelerated catalytic synthesis of oxide nanoparticles. *Nano Today.* **5** (2): 99-105.
- Ong, H.R., Khan, M.R., Chowdhury, M.N.K., Yousuf, A. & Cheng, C.K. Synthesis and characterization of CuO/C catalyst for the esterification of free fatty acid in rubber seed oil. *Fuel.* **120:** 195-201.
- Ramaswamy, A.V. 2007. Textural Characterization of Catalysts. In Vismanathan, B., Sivasanker, S. & Ramaswamy, A.V. (e.d.). *Catalysis Principles and Applications*. pp.48-70. India: Narosa Publishing House.
- Ranjbar-Karimi, R., Bazmandegan-Shamili, A., Aslani, A. & Kaviani, K. 2010. Sonochemical synthesis, characterization and thermal and optical analysis of CuO nanoparticles. *Physica B.* **405:** 3096-3100.

- Ravasio, N., Zaccheria, F. & Psaro, R. 2009. The Use of Catalysis in the Production of High-quality Biodiesel. In Barbaro, P. & Bianchini C. (e.d.). *Catalysis for Sustainable Energy Production*. pp.323-344. Weinheim: WILEY-VCH Verlag GmbH & Co.
- Rozita, Y., Brydson, R. & Scott, A.J. 2010. An investigation of commercial gamma-Al₂O₃ nanoparticles. *Journal of Physics: Conference Series*. **241**: 1-4.
- Sarkar, N., Ghosh, S.K., Bannerjee, S. & Aikat, K. 2012. Bioethanol production from agricultural wastes: An overview. *Renewable Energy*. **37** (1): 19-27.
- Sastray, G.R.K. 2008. *Bio-diesel Bio-degradable Alternative Fuel for Diesel Engines*. New Delhi: Readworthy.
- Shi, R., Wang, F., Mu, X., Li, Y., Huang, X. & Shen, W. 2009. MgO-supported Cu nanoparticles for efficient transfer dehydrogenation of primary aliphatic alcohols. *Catalysis Communications*. **11** (4): 306-309.
- Siddiqui, S.W., Unwin, P.J., Xu, Z. & Kresta, S.M. 2009. The effect of stabilizer addition and sonication on nanoparticle agglomeration in a confined impinging jet reactor. *Colloids and Surfaces A: Physicochemical and Engineering Aspects*. **350** (1-3): 38-50.
- Tantirungrotechai, J., Chotmongkolsap, P. & Pohmakotr, M. 2010. Synthesis, characterization, and activity in transesterification of mesoporous Mg-Al mixed-metal oxides. *Microporous and Mesoporous Materials*. **128**: 41-47.
- Tao, J., Yu, S. & Wu, T. 2011. Review of China's bioethanol development and a case study of fuel supply, demand and distribution of bioethanol expansion by national application of E10. *Biomass and Bioenergy*. **35** (9): 3810-3829.
- Umdu, E.S. & Seker, E. 2012. Transesterification of sunflower oil on single step sol-gel made Al₂O₃ supported CaO catalysts: effect of basic strength and basicity on turnover frequency. *Bioresource Technology*. **106**: 178-181.

- Verhé, R., Echim, C., De Greyt, W. & Stevens, C. 2011. Production of Biodiesel Via Chemical Catalytic Conversion. In Luque, R., Campelo, J. & Clark, J. (e.d.). *Handbook of Biofuels Production*, pp.97-133. United Kingdom: Woodhead Publishing.
- Vijayalakshmi, G.S., Devi, V.N.M & Prasad, P.N. 2012. *Fuels and Biofuels*. India: Agrobios.
- Vinila, V., Jacob, R., Mony, A., Nair, H.G., Issac, S., Rajan, S., Nair, A. & Isac, J. 2014: XRD studies on nano crystalline ceramic superconductor PbSrCaCuO at different treating temperature. *Crystal Structure Theory and Applications*. **3**: 1-9.
- Viswanathan, B. Kannan, S. & Deka, R.C. 2010. *Catalysts and Surface Characterization Techniques*. India: Alpha Science.
- Wang, L. & Zheng, J. 2006. Ultrasonic pretreatment of liquid NaK metal catalyst for side-chain alkenylation of *o*-xylene with 1,3-butadiene. *Ultrasonics Sonochemistry*. **13** (3): 215-219.
- Wei, D., Yang, F. & Su, E. 2010. Chemical Conversion Process for Biodiesel Production. In Cheng, J. (e.d.). *Biomass to Renewable Energy Processes*, pp. 337-435. New York: CRC Press Taylor & Francis Group.
- Yang, C., Xiao, F., Wang, J. & Su, X. 2015. 3D flower- and 2D sheet-like CuO nanostructures: microwave-assisted synthesis and application in gas sensors. *Sensors and Actuators B: Chemical*. **207**: 177-185.
- Yuan, Z., Wang, J., Wang, L., Xie, W., Chen, P., Hou, Z. & Zheng, X. 2010. Biodiesel derived glycerol hydrogenolysis to 1,2-propanediol on Cu/MgO catalyst. *Bioresource Technology*. **101**: 7088-7092.
- Zhang, L., Liu, R. & Yang, H. 2012. Preparation and sonocatalytic activity of monodisperse porous bread-like CuO via thermal decomposition of copper oxalate precursors. *Physica E*. **44** (7-8): 1592-1597.

Zhang, X., Zhang, D., Ni, X. & zheng, H. 2008. Optical and electrochemical properties of nanosized CuO via thermal decomposition of copper oxalate. *Solid-State Electronics*. **52** (2): 245-248.

Ziarati, A., Safaei-Ghom, J. & Rohani, S. 2013. Sonochemically synthesis of pyrazolones using catalyst CuI nanoparticles that was prepared by sonication. *Ultrasonication Sonochemistry*. **20** (4): 1069- 1075.